PROCESS DEVELOPMENT AND MODELLING FOR PARTICLE FORMATION OF EDIBLE FATS USING SUPERCRITICAL MELT MICRONISATION (ScMM)

P. Münüklü[1*], F. Wubbolts[1], P. J. Jansens[1]

[1]Delft University of Technology
Laboratory for Process Equipment
Leeghwaterstraat 44, 2628 CA Delft, The Netherlands

P.munuklu@wbmt.tudelft.nl

This work deals with the development of a micronisation process for edible fats based on Supercritical Melt Micronisation- technology (ScMM), also known as Particles from Gas Saturated Substrates-technology (PGSS) and the development of a model to describe the heat transfer and phase change during rapid solidification of an atomized fat droplet containing dissolved CO_2. In the PGSS process a mixture of molten edible fats is saturated with supercritical CO_2 and subsequently expanded over a nozzle. In this way micro particles can be produced with a narrow size distribution and, vital for food applications, free of solvent. A series of Experiments were performed in a continuous unit. Without CO_2 in the fat melt solid spheres were obtained. Undistorted hollow spheres to sponge like morphologies were obtained at CO_2 concentrations from 5- 50wt%, and a constant atomization pressure of 140 bar. The variations in melt temperature show spherical and hollow particles at temperatures between 60 and 80^{o}C at constant CO_2 concentration of 5wt% and an atomisation pressure of 70 bar. A numerical model was developed, which describes the solidification of one spherical droplet during the ScMM process. The subsequent steps are the isothermal solidification, undercooling and solidification of the undercooled droplet. In these steps the heat transfer influences and aerodynamic principles are modelled and presented in diagrams.

INTRODUCTION

The production of particles in micro size are traditionally produced using liquid nitrogen to make the material brittle, which is an expensive and energy consuming technique. With the PGSS method it is possible to obtain different morphologies like spherical and sponge like particles without any use of solvents or other additives except CO_2, which is a green and inexpensive solvent [1]. The developed model describes the solidification of a single droplet, by heat removal by CO_2 evaporation and entrainment of ambient air.

MATERIALS AND METHOD

The used component in this project is an edible fat and the process, which has been used is supercritical melt micronisation (ScMM) also known as PGSS (particles from gas saturated solutions).

RESULTS AND DISCUSSIONS

In Table 1 the experimental window for experiments performed under the influence of CO_2 concentration is displayed. The results of experiments at different atomization pressure and melt temperature are not included and will be presented elsewhere.

Table 1: Experimental Window of executed experiments

Exper. Nr.	$P_{atom.}$ *bar*	T_{melt} ^oC	Bulk-density g/m^3	wt.%CO_2
a)	140	80	500,0	0
b)	140	80	329,5	5
c)	140	80	355,2	10
d)	140	80	243,9	20
e)	140	80	263,6	30
f)	140	80	223,1	50

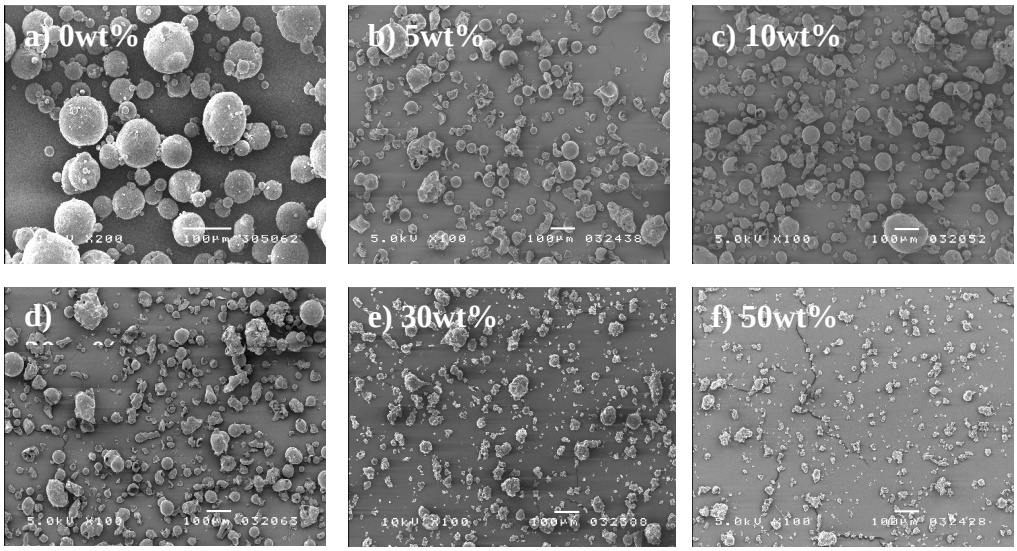

Figure1: Particles obtained at different CO_2-concentrations.
a) Completely solid spherical particles, at 0 wt% CO_2 b) Hollow particles at 5wt% CO_2, c) sponge-like Particle at 10wt % CO_2, d) Spherical hollow and agglomerates at 20wt% CO_2, e) Spherical hollow but mainly agglomerates at 30wt% CO_2, f) Sponge-like particle at 50wt.% CO_2

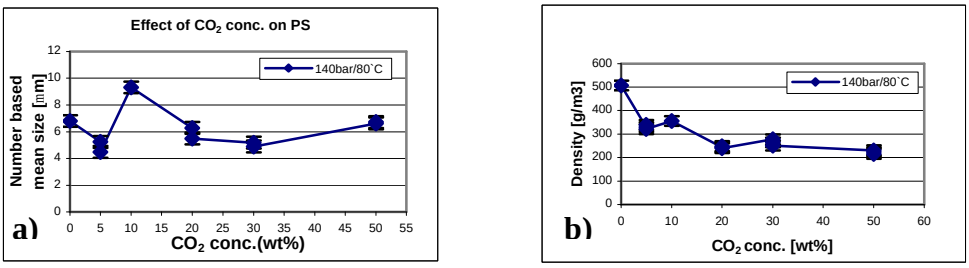

Figure2: a) Number based mean particle size versus CO_2 concentration, b) Density versus CO_2 concentration

Obviously the CO_2 concentration has an influence on the particle morphology. With increasing the CO_2 concentration the morphology of the particles transform from spherical to agglomerates, distorted or sponges like particles. From the particle size and densities measurements it can be concluded that with increasing CO_2 concentration higher than 20wt% the CO_2 does not have any significant contribution on the particle size and density. It seems to

have only a cooling effect. Experiments done at increasing melt temperature show a clear increase in density. The influence of melt temperature on the particle size and morphology was not significant. The atomization pressure has no significant influence on particle size or density. The only effect of atomization pressure was seen in the morphology, which shows with an increase in atomization pressure morphologies from spherical hollow to agglomerated sponge like particles. These droplets cool down and start to solidify due to expansion, convective cooling and CO_2 evaporation. The solidification begins at the surface of the droplet. In the absence of CO_2 completely solid particles are formed. In the presence of CO_2 inflation of the droplets occurs and hollow particles with a solid crust are formed. At relatively low melt temperatures, immediately after the droplets are formed, solidification begins and a solid crust is formed before all of the CO_2 can escape. Under such conditions, dependent on the permeability and the flexibility of the crust the droplets/particles will be deformed or even shattered leading to the observed hollow distorted or sponge like morphologies. At relatively high melt-temperatures, solidification will proceed more slowly, which on the one hand facilitates the formation of spherical (primary) particles and on the other hand promotes agglomeration since the wet droplet/particles are more likely to stick together when they collide. Similarly the effect of the CO_2-concentration in the melt can be explained in terms of competition between the solidification rate of the melt and the escape rate of CO_2. Both temperature and CO_2-concentration also have an indirect effect on the particle formation process in the sense that they have a strong effect on relevant physical properties of the melt (like viscosity, surface tension and conductivity).

MODEL

A simple model was developed to describe the heat transfer and phase change during rapid solidification of an atomized fat droplet containing dissolved CO_2. Central to this modeling is the "method of moments". The treatments have then concentrated on the simulation of those processes, which are recognized as the key factors controlling the ultimate result. These include external and internal heat transfer, nucleation and crystal growth kinetics [5]. The moment equations applicable are [3]:

$$\frac{dN}{dt} = V_L(t) I(\Delta T) \qquad (1) \qquad \frac{dA}{dt} = 2k_a L(t) G(\Delta T) \qquad (2)$$

$$\frac{dL}{dt} = N(t) G(\Delta T) \qquad (3) \qquad \frac{dM_s}{dt} = \frac{3 r_d (f_s = 1) k_v A(t) G(\Delta T)}{k_a} \qquad (4)$$

As the droplet flight continues in the powder collection vessel, the ambient air temperature changes as a result of convective heat transfer from the droplet and evaporation of CO_2. The general heat transfer equation for air of mass m_{air} is [6]:

$$m_{air} c_{pg} \frac{dT_g}{dt} = hA_d (T_d - T_g) + \frac{dm_{CO2}}{dt} C_{p,CO2} (T_d - T_g) \qquad (5)$$

If we introduce χ, such that, $c = \frac{m_{air}}{m_d}$ (6)

is the air-to-droplet mass ratio, we get after simplification of equation (5),

$$\frac{dT_g}{dt} = \frac{6h}{c[r_d(f_s)]d}\left(T_d - T_g\right) - \frac{C_{p,CO2}\left(T_d - T_g\right)}{cC_{pg}}\frac{1}{(1-x)^2}\frac{dx}{dt} \tag{7}$$

With the driving force expressed in concentration of CO2, neglecting the concentration of CO_2 in air compared to that in droplet, the rate of evaporation of CO_2 from the droplet is written as:

$$-\frac{dm_{CO_2}}{dt} = k_m A_d M_{CO_2}\left(C_{CO_2} - 0\right) \tag{8}$$

The rate of evaporation of CO_2 can be re-written in terms of the rate of change of mass fraction of CO_2 as:

$$\frac{dm_{CO2}}{dt} = \frac{d\left(\left(\frac{x}{(1-x)}\right)m_d\right)}{dt} = m_d\frac{1}{(1-x)^2}\frac{dx}{dt} \tag{9}$$

Similarly, concentration is expressed in terms of mass fraction as:

$$C_{CO2} = \frac{n_{CO2}}{V_d} = \frac{m_{CO2}}{M_{CO2}V_d} = \left(\frac{x}{1-x}\right)\frac{m_d}{V_d}\frac{1}{M_{CO2}} = \left(\frac{x}{1-x}\right)[r_d(f_s)]\frac{1}{M_{CO2}} \tag{10}$$

Substituting the results of equations(9) and (10) in equation(8) and rearranging, we get:
The mass transfer coefficient is calculated based on the two-film theory, whereby the limiting

$$\frac{dx}{dt} = -6\frac{k_m}{d}x(1-x) \tag{11}$$

mass transfer resistance determines the evaporation rate. The liquid (droplet side) mass transfer coefficient, k_L is that resulting from the penetration theory. $k_L = \sqrt{\frac{D}{pt}}$ (12)

This relation is applicable in the range, $Fo = \frac{Dt}{d^2} < 0.1$. (13)

And the outside (air side) mass transfer coefficient, k_V is calculated from the relation [4]:

$$Sh = 2 + 0.79\,\mathrm{Re}^{1/2}\,Sc^{1/3} \tag{14}$$

Where, $Sh = \frac{k_V d}{D_V}$, is the Sherwood number, and $Sc = \frac{h_g}{r_g D_V}$ is the Schmidt number [4].

The most significant results of the solutions of the differential equations discussed so far are presented as graphs in figs.3 and 4, where the air to droplet temperature profile and the droplet solidification rate at different CO_2 concentration are shown.

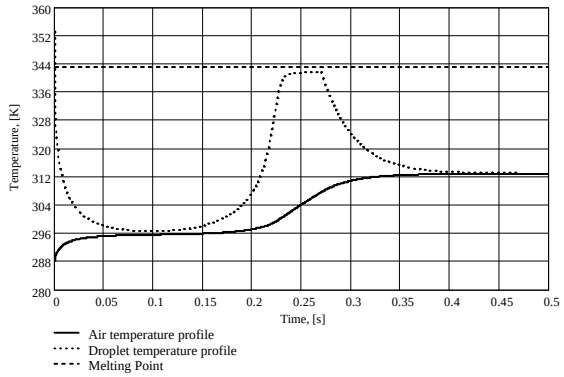

Figure 3: Air to Droplet temperature profile different

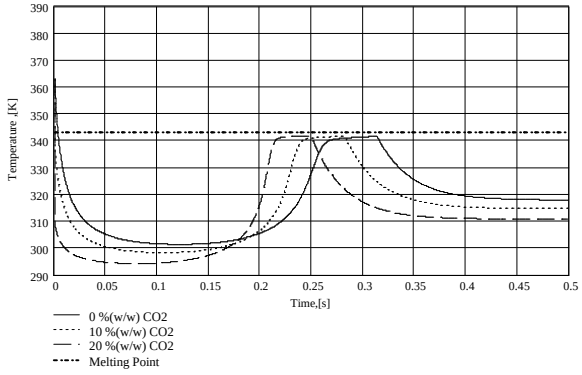

Figure 4: Droplet solidification rate at CO_2 concentrations

Fig.3 shows a typical result of the relationship between the thermal profiles of the droplet and the ambient air. It shown that there is a rapid decrease in droplet temperature associated with a relatively rapid increase in ambient air temperature at the beginning of the process. This rapid decrease in droplet temperature may be attributed to two factors. First, the CO_2 evaporates very fast at the beginning which results in rapid cooling of the droplet as it takes heat from the droplet for its evaporation. Second, there is a high convective heat transfer from the droplet to the ambient air due primarily to the higher driving force for heat transfer as a result of higher droplet temperatures coupled with lower ambient air temperatures. However, this initial situation is almost brought to a halt as the two temperature profiles come close to each other leaving little driving force for heat transfer. This results in a temporary isothermal condition with respect to both the droplet and the ambient air. It can be said there is a brief balance between rise in heat energy of the droplet as a result of initial, low level solidification, and heat loss to the ambient air through the little remaining driving force. However, after e certain time the number of nuclei increases, which increases the solidification rate. This results in a relatively rapid increase in droplet temperature. This increase will have two notable effects. First, the undercooling is decreasing the nucleation and growth rates of crystals; secondly, the driving force for heat transfer between the droplet and the air increases. These two situations have opposite effects on the thermal state of the droplet and a certain temperature is established after some time. This situation becomes evident from the constant droplet temperature, which is close to the normal melting, point. As the solidification process is completed, there will be no more latent heat release and the droplet temperature only cools as any solid from which heat is continuously being withdrawn. Finally, the temperature of the droplet and that of the ambient air come together after all possible heat is extracted from the droplet. As seen from the figure 4, as the initial CO_2 concentration increases, the rate of drop in droplet temperature at the beginning of the process increases which results in both in higher cooling rate and deeper undercooling. This higher undercooling is in turn reflected in higher recalescence rate, and the temperatures of droplets starting with more CO_2 are shown to overtake those starting with less CO_2. The overall effect is lower solidification times in droplets starting with more CO_2.

CONCLUSION

The shape and the size of the formed particles can be manipulated by the temperature of the melt and by the CO_2 /melt ratio. The temperature in the collection vessel should be kept low to suppress agglomeration. Using a novel equipment configuration it has become possible to control the particle morphology propose. A continuous ScMM-process for edible fat was successfully developed which yields hollow or solid spheres, in the size range 4 – 9 micron and a powder bulk density between 215 – 500 g/m^3. The model shows us the influence of certain parameters. Higher initial CO_2 concentration, lower initial droplet temperature, and lower initial air temperature are shown to facilitate the rapid cooling and solidification of droplets. The CO_2 concentration in the feed mixture turned out to be the governing operating variable. A simple model for the particle solidification was presented but it is not (yet) possible to link model-predictions to experimental results directly.

REFERENCES:

[1] P. MUNUKLU, F.E. WUBBOLTS, P.J. JANSENS, ASC Symposium Series 860, **2003**

[2] LAVERNIA, E.J., AND WU, Y., Spray atomization and deposition, **1996**

[3] F.E, WUBBOLTS, E.E., Supercritical Crystallization: Volatile Components As (anti-) Solvents, **2000**

[4] SKELLAND, A.H.P., Diffusional mass transfer, **1952**

[5] CLYNE, T.W., Numerical treatment of Rapid solidification, Metall.Trans. B, **15 B**, 369, **1984**

[6] PERRY, R.H., Perry's Chemical Engineering's Handbook, 6th edition, **1984**

Symbol	Description	Unit
A	Total external area of crystal entities in the droplet	m^2
$C_{p,d}$	Constant pressure heat capacity of droplet	J/(mol.K)
$C_{p,g}$	Constant pressure heat capacity of Gas	J/(mol.K)
d	Droplet Diameter	m
d_m	The effective molecular diameter	m
D_v	Diffusivity of CO_2 in air	m^2/s
$f(\theta)$	Nucleate potency	[-]
f_s	Solid fraction	[-]
G	Crystal growth rate	M/s
h	Convective heat transfer coefficient	$W/(m^2 K)$
I	Nucleation rate	$\#/(m^3.s)$
k_a	Surface shape factor of crystals	[-]
k_g	Thermal Conductivity of atomization Gas	W/(m.K)
k_L	Droplet side coefficient of mass transfer	m/s
k_m	Mass transfer coefficient	m/s
k_V	Air side coefficient of mass transfer	m/s
L	Total length of crystal entities	m
m_{CO2}	Total mass of CO_2 in the droplet	kg
m_d	Total mass of droplet	kg
m_{air}	Mass of ambient air	kg
N	Total number of crystal sites (nuclei)	[#]
n_{CO2}	Number of moles of CO_2	moles
t	Time	S
T	Temperarture	K
T_d	Droplet temperature	K
T_g	Temperature of Atomization Gas	K
A_d	Volume of Droplet	m^3
v_{do}	Release velocity of droplet from the nozzle	m/s
V_m	Volume of molecule	m^3/molecule
V_L	Volume of the liquid portion of a droplet	m^3
χ	Ambient air-to-droplet mass ratio	[-]
ρ_g	Density of atomization Gas	kg/m^3
ρ_d	Density of droplet	kg/m^3
η_g	Dynamic Viscosity of Ambient Gas	Pa.s
ΔT	Undercooling	K